CHEMISTRY
A European Journal

A Journal of
ChemPubSoc Europe

Accepted Article

Title: Visible light Direct Conversion of Ethanol to 1,1-Diethoxyethane and Hydrogen over Non-Precious Metal Photocatalyst

Authors: Yuguang Chao, Wenqin Zhang, Xuemei Wu, Nana Gong, Zhihong Bi, Yunqin Li, Jianfeng Zheng, Zhenping Zhu, and Yisheng Tan

To be cited as: *Chem. Eur. J.* 10.1002/chem.201804664

Link to VoR: http://dx.doi.org/10.1002/chem.201804664

Supported by
ACES

WILEY-VCH

WILEY-VCH

DOI: 10.1002/((please add manuscript number))
Article type: Communication

Visible light Direct Conversion of Ethanol to 1,1-Diethoxyethane and Hydrogen over Non-Precious Metal Photocatalyst

Yuguang Chao, Wenqin Zhang, Xuemei Wu, Nana Gong, Zhihong Bi, Yunqin Li, Jianfeng Zheng, Zhenping Zhu and Yisheng Tan**

Y. Chao, W. Zhang, X. Wu, N. Gong, Y. Li, Prof. J. Zheng, Prof. Z. Zhu, Prof. Y. Tan
State Key Laboratory of Coal Conversion, Institute of Coal Chemistry, Chinese Academy of Sciences, Taiyuan, 030001, China.

Y. Chao, X. Wu, N. Gong, Z. Bi
University of Chinese Academy of Sciences, Beijing, 100049, P. R. China.

Z. Bi
Key Laboratory of Carbon Material, Institute of Coal Chemistry, Chinese Academy of Sciences, Taiyuan 030001, PR China

Keywords: visible light; non-precious metal; ethanol; photocatalytic; 1,1-diethoxyethane

Abstract: Converting renewable biomass and their derivatives into chemicals and fuels has received much attention to reduce the dependence on fossil resources. We report an efficient and green atom economic process achieved over non-precious metal CdS/Ni-MoS_2 catalytic under visible light. Renewable H_2 and value-added 1,1-diethoxyethane are obtained at the same time by photocatalytic water splitting with ethanol as sacrificial agent. The system displays an excellent production rate and high selectivity of 1,1-diethoxyethane, 52.1 mmol g^{-1} h^{-1} and 99.2%, respectively. In-situ electron spin resonance, photoluminescence spectroscopy and transient photocurrent responses are conducted to investigate the mechanism. This study provides a promising strategy for atomic green economy application of bio-ethanol.

The conversion of solar energy to electric energy and chemical energy has become the hot topic of research in today's society.[1-10] Converting water into renewable hydrogen (H_2) fuel by photocatalytic water splitting, inspired by natural photosynthesis, has been considered as a promising avenue to settle the energy and environmental issues, attracting ebullient attention in recent

decades.[11-15] However, sacrificial agent (e.g., methanol and ethanol) need adding to improve the efficiency of solar-to-H_2 in most reaction systems.[16-22] The main function of these sacrificial agents is capturing photogenerated holes to accelerate water oxidation kinetics. Unfortunately, the majority of sacrificial agent is oxidized to CO or CO_2, which is harmful to environment.[23,24] As one of the most important bio-alcohols, ethanol contains 13.04 wt% of hydrogen, being perceived as a potential hydrogen storage medium, obtained from biomass fermentation.[25] Therefore, photocatalytic ethanol dehydrogenation, converting into value-added chemicals without CO_x release, is a logical strategy to solve the problems above.

1,1-diethoxyethane (DEE), a value-added derivative product of the ethanol selective oxidation, has drew intense attention recently, due to its multidisciplinary applications in pharmaceuticals, fuel additive, fragrance industry and intermediate for chemical synthesis.[26-28] Particularly, DEE is regarded as a remarkable additive to replace ethanol in fuel, for it can keep or increase the cetane number of the fuel[29] and combust the resulting mixtures more drastically.[30] Interestingly, as an additive into fuel, DEE can also drastically inhibit the emission of nitrogen oxide.[31] All these features indicate that the conversion into DEE is a promising channel for the rational utilization of bioethanol. However, the traditional conversion of ethanol into DEE process requires two steps: ethanol was selectively oxidized to aldehyde and then acid catalyzed aldehyde–ethanol acetalization as DEE.[31-33] In this traditional process, the oxidation step is highly damaging to environment, the system is really complex and strict in terms of reactor equipment. Therefore, it is urgent requirement for exploiting a simple method to convert ethanol to DEE green and economically.

Photocatalytic acetal reaction supplies a novel strategy to convert ethanol into acetal effectively. Our group achieved visible light driven methanol dehydrogenation–acetalization, converting into 1,1-dimethoxymethane and H_2 over noble metal-free photocatalyst CdS/Ni_2P nanostructured in one step.[34] Zhang and coworkers demonstrated that Pd/TiO_2 nanostructures are highly photoactive for the dehydrogenation C-O coupling of ethanol into DEE.[31,35,36] Xu's group reported that the

decoration of Pd nanocubes onto TiO_2 nanosheets allows simultaneous DEE production and H_2 evolution under ultraviolet light.[37] However, the only ultraviolet light response of TiO_2 and the expensive noble metal co-catalysts restrict the large-scale actual application of photocatalytic acetal reactions.

In this work, ethanol is converted into DEE and H_2 over non-precious metals CdS nanorods/Ni-MoS_2 nanosheets via photocatalytic dehydrogenation–acetalization under visible light. A small amount of sulphuric acid exists in the reaction system. The acid can not only drive the dehydrogenation of ethanol, but also catalyze the acetalization reaction. The rate and selectively of photocatalytic DEE evolution reaches 52.1 mmol g^{-1} h^{-1} and 99.2%, respectively, while the H^+ concentration is 30 mM. Simultaneously, the trace acid in the reaction system does not corrode the catalyst and glass reactor at all.

The well shaped CdS nanorods were synthesized on the basis of previously reported method,[38] serving as photocatalyst. The Ni-MoS_2 nanosheets were loaded onto CdS nanorods in-situ through the solvothermal reaction with L-cysteine, $Na_2MoO_4 \cdot 2H_2O$ and $Ni(NO_3) \cdot 6H_2O$ as precursors at 200 ℃ for 30 h. The field-emission scanning electron microscopy (FESEM) (**Figures 1a** and **S1**) and transmission electron microscopy (TEM) images (**Figures S2a** and **S2b**) shown that the as-prepared CdS was uniform well-shaped 1D nanorods with the average diameter of about 30-40 nm. **Figure 1b** and **1c** clearly presented the FESEM and TEM images of CdS nanorods after growing Ni-MoS_2 nanosheets on their surface, and the nanorods kept their 1D geometries. High-resolution transmission electron microscopy (HRTEM) image (**Figure 1d**) shown a lattice spacing of about 0.34 nm consistent with the (002) plane of hexagonal CdS, and lattice spacing of about 0.64 nm, coinciding with the (002) plane of Ni-MoS_2 nanosheets. X-ray diffraction (XRD) was carried out to investigate the crystal structures of the as-made photocatalysts nanostructure. All characteristic peaks were well in agreement with the standard card of hexagonal CdS (JCPDS card No. 41-1049) (**Figure S3**). Nevertheless, no obvious diffraction peaks were attributed to Ni-MoS_2 in the XRD patterns and

no significant diffraction peaks were different from those of the CdS nanorods after the co-catalyst loaded, probably due to the relatively small amount of Ni-MoS_2 distribution and too strong diffraction peaks of the CdS nanorods.[39-41] In addition, we specialized in the synthesis of Ni-MoS_2 without CdS nanorods addition, and XRD pattern unveiled that the nickel was doped in the MoS_2, due to no obvious characteristic peaks of NiS (**Figure S4**), which was in agreement with a previous report.[42]

X-ray photoelectron spectroscopy (XPS) was employed for investigating the chemical state of the as-made CdS/Ni-MoS_2 nanostructure. The survey scan displayed the existence of Cd, S, Mo, Ni elements in the as-prepared CdS/Ni-MoS_2 (**Figure S5a**). The binding energy peaks of Mo $3d_{3/2}$ and Mo $3d_{5/2}$ were located at 231.4 and 228.2 eV (**Figure S5b**), respectively, while that of S $2p_{3/2}$ and S $2p_{1/2}$ peaks located at 161.1 and 162.4 eV (**Figure S5c**). These results suggested that the valence states of the Mo and S elements in the final Ni-MoS_2 nanosheets were Mo^{4+} and S^{2-}.[43,44] It can be observed from the Ni 2p spectra shown in **Figure S5d** that the Ni $2p_{3/2}$ binding energy of 853.4 eV corresponded to the Ni in the Ni–Mo–S structure.[45] The UV–vis diffuse reflectance spectra (DRS) of the as synthesized samples were shown in **Figure S6**, and all the photocatalysts samples performed strong absorption in the region from 200–520 nm, assigning to the intrinsic bandgap absorption of CdS nanorods. Notability, loading the Ni-MoS_2 co-catalysts onto the surface of CdS nanorods could obviously increase the absorption of samples in visible light region of 520 to 800 nm. This was beneficial to improve the activity of photocatalytic ethanol dehydrogenation.

The photocatalytic ethanol dehydrogenation coupling over the CdS/Ni-MoS_2 nanocomposites had been performed in ethanol media (containing different concentration of H^+) under visible light irradiation ($\lambda > 420$ nm). Different amounts of co-catalyst Ni-MoS_2 nanosheets had been covered on CdS nanorods to investigate the optimum weight percent of Ni-MoS_2 to enhance the photoactivity of catalysts with the concentration of H^+ is 30 mM, as shown in **Figure 2a**. The photocatalytic H_2 production exhibited a improved tendency with increasing Ni-MoS_2 content. Nevertheless, the

excess co-catalyst might reduce the light absorption of CdS nanorods and served as recombination centre for charge carriers, indicating that an suitable co-catalyst content is of importance for optimizing the photo-activity of $CdS/NiMoS_2$.[34] Thereby, the photocatalyst achieved a optimal value at the weight content of 7 wt%, the H_2 production rate reaches an optimal value of up to 52.1 mmol g^{-1} h^{-1}, and this result was in accordance with the UV-vis spectrum (**Figure S6**). The durability of $CdS/NiMoS_2$ catalyst was studied by four consecutive cycles with each cycle of four hour under visible light irradiation (**Figure 2b**). At the end of each run, the reactor was evacuated and then refilled with Ar, but the catalyst was not treated. No obvious deactivation was observed within four repeated cycles of photocatalysis, and the crystalline structures of $CdS/NiMoS_2$ photocatalyst before and after 4 cycles photocatalytic reaction had no significant change (**Figure S7**), indicating the outstanding photo-stability of the $CdS/NiMoS_2$ under acid condition and potential for long-term photocatalytic actual applications.

During photocatalytic H_2 evolution from ethanol dissociation, ethanol could be converted into value-added 1,1-diethoxyethane (DEE) in the presence of acid (sulphuric acid). The chemical compositions of the liquid products were analyzed by utilizing GC-MS, as shown in **Figure S8** and **Figure S9**. The main liquid phase products were DEE and aldehyde. As H^+ played important roles in catalyzing the acetal reaction,[35,46] we investigated the effect with various H^+ concentrations on the production rate and the selectivity of DEE. As shown in **Figure 3a**, the rate of DEE production was increasing with the increase of H^+ concentration, and it was worth noting that the rate of DEE production can reach 52.1 mmol g^{-1} h^{-1} in 30 mM H^+ ethanol solution. However, the selectively had no obvious change at the different H^+ concentration (**Figure 3b**), which maintains 99.2%. The high selectively was ascribed to the rapid reaction of ethanol with the product of the dehydrogenation of ethanol in the presence of H^+. In addition, the yield of ethanol conversion can reach to 5% after 12 hours reaction. Interesting, we did not detect the any carbon oxide in the photocatalysis process, and the only by-product was aldehyde. Moreover, taking the selectivity of DEE into consideration, the

rate of DEE evolution was similar to that of H_2, maintaining a rate ratio of 1 : 1, indicating the photocatalytic process proceeded nearly by following the chemical equation shown below, according with the previous report:[25]

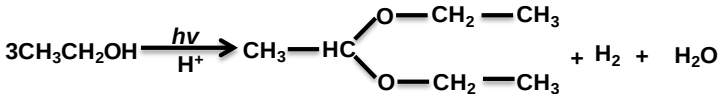

In addition, the effect of acid species added in ethanol solution was also investigated. It is clearly visible that, when the H^+ ions were supplied by HCl aqueous solution (36-38%), both the rate and selectively of DMM production decreased (**Figure S10**). The reason was the fast hydrolysis of DEE to acetaldehyde (inverse reaction) in the presence of water, which was introducd by hydrochloric acid aqueous solution, thereby HCl aqueous solution was not a ideal medium to adjust the pH of reaction system.[31,34] Moreover, when no acid was added in the ethanol solution, the rate of photocatalytic H_2 evolution decreased sharply and no DEE was detected in liquid product. The ethanol dehydrogenation and conversion into butane-2,3-diol and aldehyde (**Figures S11** and **S12**), and the selectivity of butane-2,3-diol and aldehyde were 46.8% and 53.2%, respectively. This photocatalytic ethanol dehydrated path was consistent with the previous report.[35,47,48] This process also exhibited an excellent photocatalytic H_2 evolution stability, having no obvious decrease as long as for 18 h (**Figure S13**).

To exploring the mechanism of photocatalytic ethanol converting into DEE and H_2, an in-situ electron spin resonance (ESR) was conducted for the analysis of the reaction intermediates radicals. **Figure 4** displayed the ESR spectrum during the process of photocatalytic ethanol dehydrogenation coupling reaction by using 5, 5-dimethyl-1-pyrroline N-oxide (DMPO, 0.05 M) capturing the reaction intermediates radicals over the CdS/NMS7 photocatalyst. The ESR result shown the existence of hydroxyl ethyl radical $\cdot(CHOHCH_3)$ (a_N = 15.4, a_H = 22) in the photocatalysis process, which was identical with the Zhang's report.[36] This intermediate should be formed in dissociating one H atom from ethanol (α-H) by the oxidation of photo-generation holes. This radical continued to

dissociate another α-H by the further oxidation, forming one stable aldehyde molecule. Meanwhile, no ethoxy radical was detected, indicating the dehydrogenation occurring at α-H, but not O-H. Thereby, the value-added DEE could be obtained from the reaction of the generated aldehyde and ethanol under acid condition.

Photoluminescence (PL) spectroscopy and transient photocurrent responses were considered to powerful techniques for investigating the separation and transfer of charge carriers. **Fig. 5a** shown two distinct emission bands at ca. 530 nm and 640 nm, which could be attributed to near-band-edge emission and the excess of sulfur or core defects on the nanorod surfaces, respectively. The PL emission intensity exhibited an obvious decrease as the co-catalyst Ni-MoS_2 loaded, indicating that the co-catalyst Ni-MoS_2 can improve the separation efficiency of photo-generated charge carries. Notably, the CdS/NMS7 exhibited the optimal performance to enhance the separation of charge carriers. The transient photocurrent responses were performed with interval 10 s periodic light on/off cycle under visible light irradiation (**Fig. 5b**). The CdS/NMS7 exhibited the highest cathodic photocurrent among all the as-prepared samples, even twice higher than the current of bare CdS nanordos. The addition of co-catalyst Ni-MoS_2 accelerated the electron separation and transfer process, resulting in higher performance of photocatalytic ethanol dehydrogenation.

The probable mechanism of visible light-driven ethanol dehydrogenation-acetalization reaction can be summarized by above results. CdS nanorods were excited by visible light, producing the photo-generated charge carriers. The electron-holes pairs recombined quickly without the co-catalyst loaded resulting relatively poor activity. When Ni-MoS_2 was covered on the surface of CdS nanorods, the charge carrier could be separated and transferred effectively. Therefore, the holes on the CdS nanorods were easy to oxidize CH_3CH_2OH to generate the hydroxyl ethyl radical intermediate, $^{\cdot}CH(OH)CH_3$. The intermediate were further oxidized to aldehyde (CH_3CHO) because of their dynamical instability property. Then the generated aldehyde reacts with ethanol rapidly to form DEE under acidic conditions, while no acetic acid was detected and no CO_x was released in this reaction.

Meanwhile, the generated two protons transfer to the surface of the Ni-MoS_2 nanosheets, followed by reducing to H_2 by the photo-generation electrons at the conduction band of the CdS nanorods. Therefore, only value-added DEE and H_2 generated in this photocatalytic ethanol dehydrogenation-acetalization reaction, avoiding the environmental pollution occurring in traditional acid-catalyzed acetalization processes.

In summary, photocatalytic ethanol dehydrogenation-acetalization reaction was achieved in one step on non-precious metals CdS/Ni-MoS_2 catalyst by visible light driven for the first time. The value-added DEE and sustainable H_2 were obtained in this atom economic green avenue. The optimal photocatalyst CdS/NSM7 composite exhibits excellent rate and selectivity of DEE evolution under a suitable acid condition ($[H^+]$ = 30 mM), which is 52.1 mmol g^{-1} h^{-1} and 99.2%, respectively. There is no CO or CO_2 detected in the gas phase products, avoiding the environmental pollution. This work explores a viable strategy for the direct efficient conversion of ethanol into value-added DEE and sustainable H_2 by visible light driven, and provides a promising strategy for atomic economy green application of bio-ethanol.

Supporting Information
Supporting Information is available from the Wiley Online Library or from the author.

Acknowledgements
This work was financially supported by the National Natural Science Foundation of China (91545116 and 21573269).

Received: ((will be filled in by the editorial staff))
Revised: ((will be filled in by the editorial staff))
Published online: ((will be filled in by the editorial staff))

References

[1] R. Chen, S. Pang, H. An, J. Zhu, S. Ye, Y. Gao, F. Fan, C. Li, *Nat. Energy* **2018**, 8, 655.

[2] A. Abate, J. P. Correa-Baena, M. Saliba, M. S. Su'ait, F. Bella, *Chem. Eur. J.* **2018**, 24, 3083.

[3] S. H. Li, N. Zhang, X. Xie, R. Luque, Y.-J. Xu, *Angew. Chem. Int. Ed.* **2018**.

[4] F. Bella, M. Imperiyka, A. Ahmad, *J. Photoch. Photobio. A*, **2014**, 73.

[5] A. Sacco, F. Bella, S. De La Pierre, M. Castellino, S. Bianco, R. Bongiovanni, C. F. Pirri, *Chemphyschem*, **2015**, 5, 960.

[6] G. Zhao, Y. Sun, W. Zhou, X. Wang, K. Chang, G. Liu, H. Liu, T. Kako, J. Ye, *Adv. Mater.* **2017**, 40.

[7] F. Bella, P. Renzi, C. Cavallo, C. Gerbaldi, *Chem. Eur. J.* **2018**, 47, 12183.

[8] X. Wang, H. Wang, H. Zhang, W. Yu, X. Wang, Y. Zhao, X. Zong, C. Li, *ACS Energy Lett.* **2018**, 5, 1159.

[9] D. Ompong, J. Singh, *Organic Electronics* **2018**, 104.

[10] F. Bella, A. Sacco, G. Massaglia, A. Chiodoni, C. F. Pirri, M. Quaglio, *Nanoscale* **2015**, 28, 12010.

[11] P. Zhou, J. Lai, Y. Tang, Y. Chao, F. Lin, S. Guo, *Appl. Catal. B: Environ.* **2018**, 161.

[12] Y. Chao, J. Zheng, H. Zhang, Y. Ma, F. Li, Y. Tan, Z. Zhu, *Energy Technol.* **2018.**

[13] N.S. Lewis, D.G. Nocera, *Proc. Natl. Acad. Sci. U.S.A.* **2006**, 103, 15729.

[14] Y. Chao, J. Zheng, H. Zhang, F. Li, F. Yan, Y. Tan, Z. Zhu, *Chem. Eng. J.* **2018**, 281.

[15] J. Ran, G. Gao, F. T. Li, T. Y. Ma, A. Du, S. Z. Qiao, *Nat. Commun.* **2017**, 13907.

[16] Y. Honda, H. Hagiwara, S. Ida, T. Ishihara, *Angew. Chem. Int. Ed.* **2016**, 28, 8045.

[17] L. Li, J. Yan, T. Wang, Z. J. Zhao, J. Zhang, J. Gong, N. Guan, *Nat. Commun.* 2015, 5881.

[18] C. Xu, W. Yang, Q. Guo, D. Dai, M. Chen, X. Yang, *J. Am. Chem. Soc.* **2014**, 2, 602.

[19] G. Liu, L. Ma, L.-C. Yin, G. Wan, H. Zhu, C. Zhen, Y. Yang, Y. Liang, J. Tan, H.-M. Cheng, *Joule* **2018**, 6, 1095.

[20] X. Zhou, E. M. Zolnhofer, N. T. Nguyen, N. Liu, K. Meyer, P. Schmuki, *Angew. Chem. Int. Ed.* **2015**, 45, 13385.

[21] F. Niu, S. Shen, L. Guo, *J. Catal.* **2016**, 141.

[22] S. Mohajernia, S. Hejazi, A. Mazare, N.T. Nguyen, P. Schmuki, *Chem. Eur. J.* **2017**, 23,12406.

[23] J. Saavedra, H. A. Doan, C.J. Pursell, L.C. Grabow, B.D. Chandler, *Science*, **2014**, 345.

[24] Z. Liu, Z. Yin, C. Cox, M. Bosman, X. Qian, N. Li, H. Zhao, Y. Du, J. Li, D.G. Nocera, *Sci. Adv.* **2016**; 2 : e1501425

[25] J. C. Serrano-Ruiz, R. Luque, A. Sepulveda-Escribano, *Chem. Soc. Rev.* **2011**, 11, 5266.

[26] F. Frusteri, L. Spadaro, C. Beatrice, C. Guido, *Chem. Eng. J.* **2007**, 1-3, 239.

[27] F.A.J. Meskens, *Synthesis* **1981**, 7, 501.

[28] M.R. Capeletti, L. Balzanob, G. Puente, M. Laborde, U. Sedran, *Appl. Catal. A: Gen.* **2000**, 198, L1.

[29] K. Bonhoff, F. Obenaus, *Pat. DE*, **1980**, 411.

[30] K. Oppenlaender, F. Merger, R. Strickler, F. Hovemann, H. Schmidt, K. Starke, K. Stork, W. Vodrazka, *Eur. Pat.*, **1980**, 922.

[31] H. Zhang, Y. Wu, L. Li, Z. Zhu, *ChemSusChem* **2015**, 7, 1226.

[32] T. W. Green, *Protective Groups in Organic Synthesis Wiley*, New York,**1981**.

[33] R. Morrison, R. Boyd, *Organic chemistry*, 4th ed., Allyn and Bacon, London, **1983**.

[34] Y. Chao, J. Lai, Y. Yang, P. Zhou, Y. Zhang, Z. Mu, S. Li, J. Zheng, Z. Zhu, Y. Tan, Catal. Sci. Technol. 2018, 13, 3372.

[35] H. Zhang, Z. Zhu, Y. Wu, T. Zhao, L. Li, *Green. Chem*. **2014**, 9, 4076.

[36] H. Zhang, W. Zhang, M. Zhao, P. Yang, Z. Zhu, *Chem. Commun.* **2017**, 9, 1518.

[37] B. Weng; Q. Quan; Y.-J. Xu, *J. Mater. Chem. A* **2016**, 47, 18366.

[38] J. S. Jang, U. A. Joshi, J. S. Lee, *J. Phys. Chem. C* **2007**, 111, 13280.

[39] B. Han, S. Liu, N. Zhang, Y.-J. Xu, Z.-R. Tang, *Appl. Catal. B: Environ.* **2017**, 298.

[40] S. Cao, Y. Chen, C.-C. Hou, X.-J. Lv, W.-F. Fu, *J. Mater. Chem. A* **2015**, 11, 6096.

[41] H. Park, D. A. Reddy, Y. Kim, S. Lee, R. Ma, T. K. Kim, *Chemistry* **2017**, 53, 13112.

[42] Y. Chao, J. Zheng, J. Chen, Z. Wang, S. Jia, H. Zhang, Z. Zhu, *Catal. Sci. Technol.* **2017**, 13, 2798.

[43] W. Lai, Z. Chen, J. Zhu, L. Yang, J. Zheng, X. Yi, W. Fang, *Nanoscale* **2016**, 6, 3823.

[44] Z. Yang, D. Gao, J. Zhang, Q. Xu, S. Shi, K. Tao, D. Xue, *Nanoscale* **2015**, 2, 650.

[45] W. Park, J. Baik, T.-Y. Kim, K. Cho, W.-K. Hong, H.-J. Shin, T. Lee, *ACS Nano*, **2014**, 8, 4961.

[46] T. Simon, N. Bouchonville, M. J. Berr, A. Vaneski, A. Adrovic, D. Volbers, R. Wyrwich, M. Doblinger, A. S. Susha, A. L. Rogach, F. Jackel, J. K. Stolarczyk, J. Feldmann, *Nat. Mater.* **2014**, 11, 1013.

[47] H. Lu, J. Zhao, L. Li, L. Gong, J. Zheng, L. Zhang, Z. Wang, J. Zhang, Z. Zhu, *Energy Environ. Sci.*, **2011**, 4, 3384.

[48] P. Yang, J. Zhao, B. Cao, L. Li, Z. Wang, X. Tian, S. Jia, Z. Zhu, *ChemCatChem*, **2015**, 7,2384.

10.1002/chem.201804664

WILEY-VCH

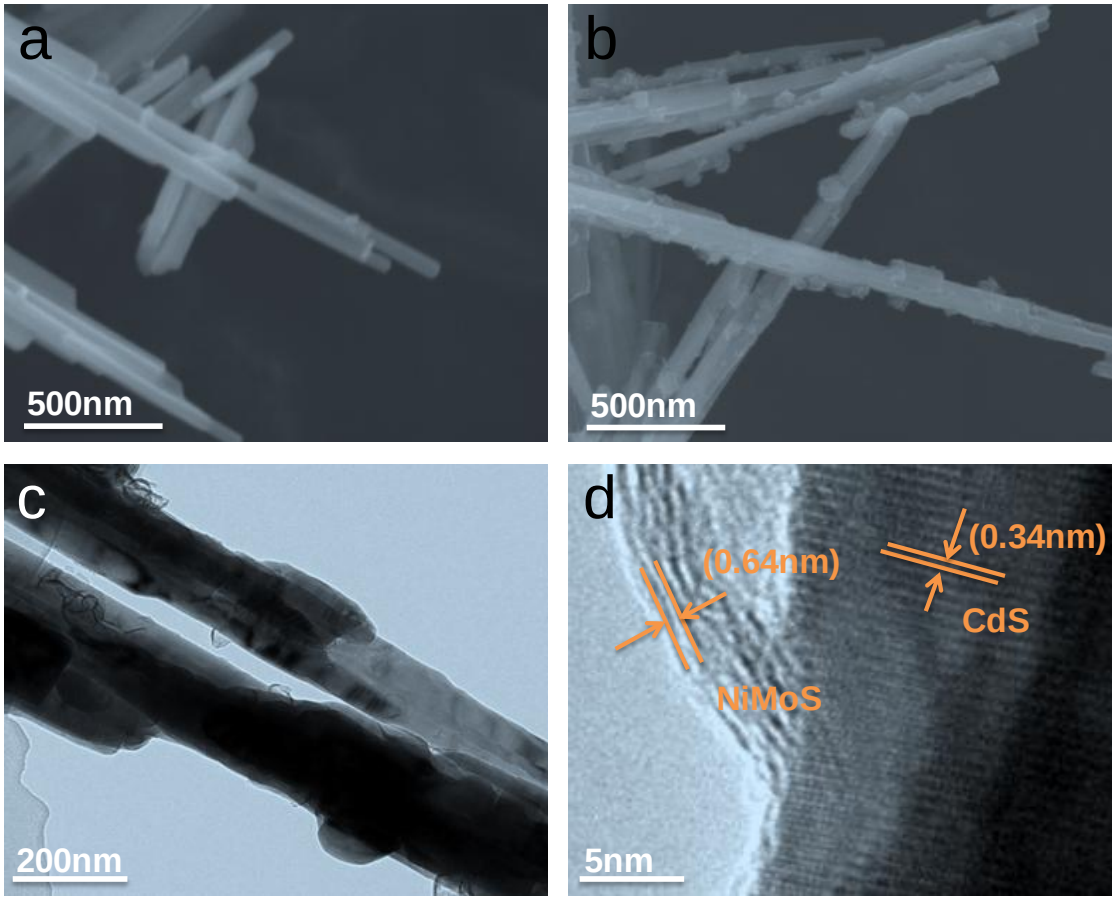

Figure 1. (a) Typical SEM image of blank CdS nanorods, (b) SEM images of as-prepared samples CdS/NiMoS-7 nanostructure. (b) and (d) TEM and HRTEM images of as-prepared CdS/NiMoS-7 nanostructure.

10.1002/chem.201804664

WILEY-VCH

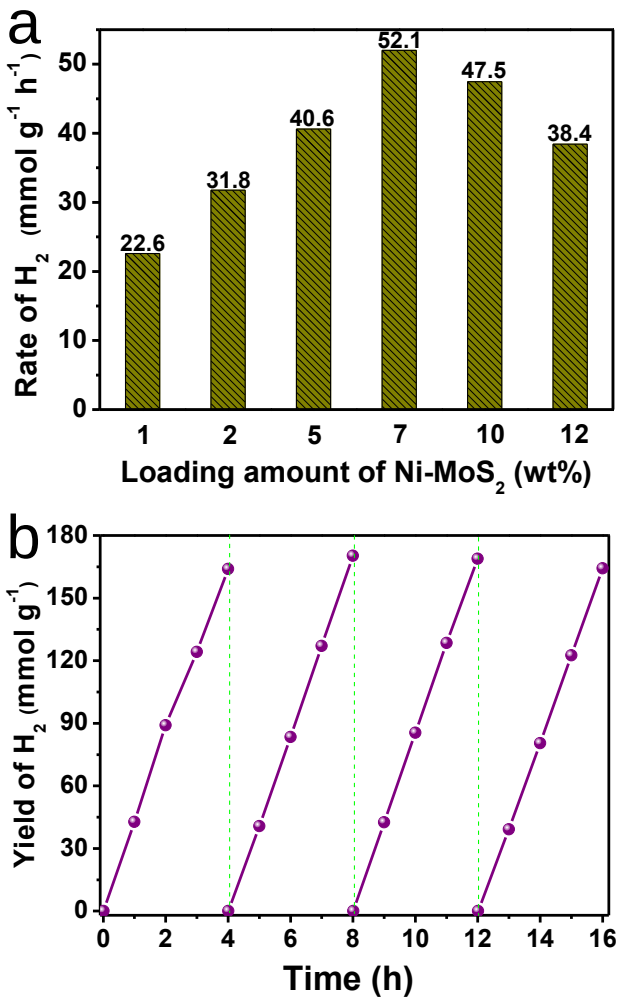

Figure 2. (a) The rates of photocatalytic ethanol dehydrogenation over CdS/Ni-MoS_2 samples with different Ni-MoS_2 loading amounts (c(H^+) = 40 mM), (b) Photocatalytic ethanol dehydrogenation cycling test (evacuation every 4 h) for CdS/NMS7 samples under visible-light (λ > 420 nm, 300 W Xe lamp).

10.1002/chem.201804664

WILEY-VCH

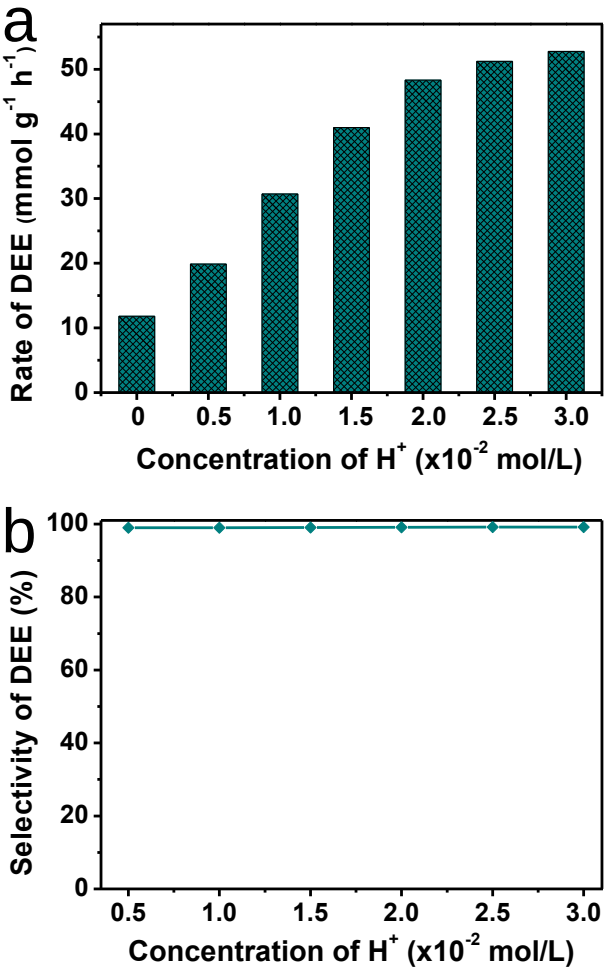

Figure 3. (a) The rates of photocatalytic ethanol dehydrogenation at different H^+ concentration, (b) The effect of H^+ concentration on selectivity of DEE.

10.1002/chem.201804664

WILEY-VCH

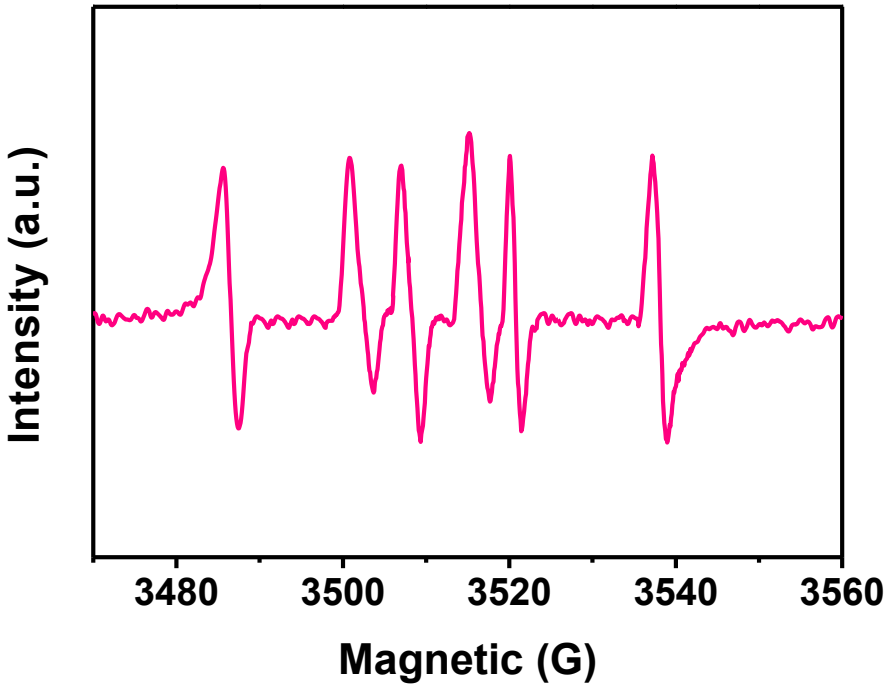

Figure 4. In-situ ESR spectrum in the process of ethanol degydrogenation over CdS/NMS7 catalyst in the presence of DMPO (a spin-trapping agent) under visible light irradiation (30 mM H^+).

10.1002/chem.201804664

WILEY-VCH

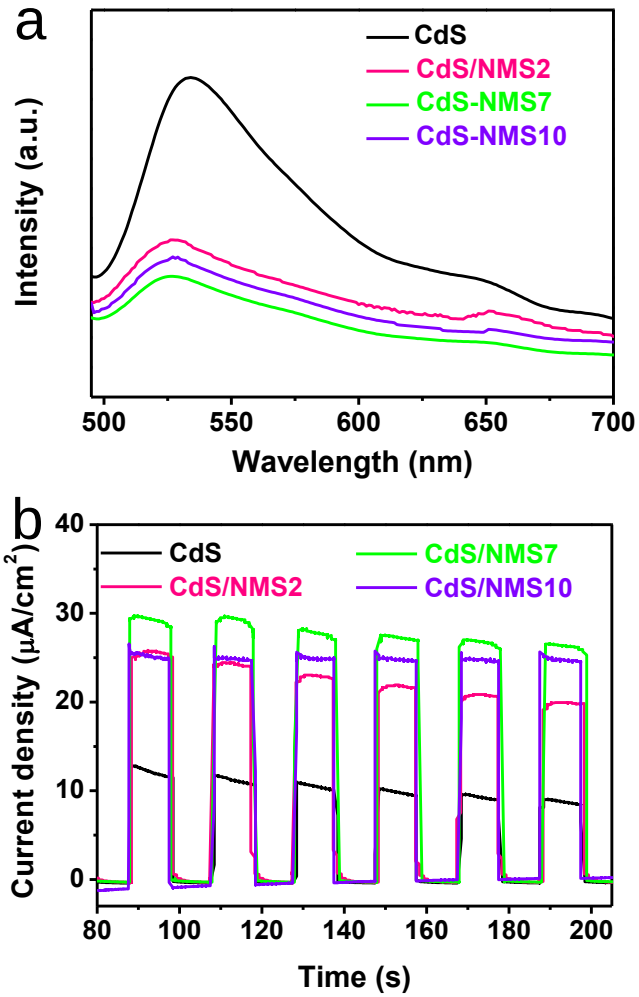

Figure 5. (a) Transient photocurrent responses and (b) photoluminescence spectra with an excitation wavelength of 420 nm of the as-prepared photocatalysts samples.

10.1002/chem.201804664

WILEY-VCH

The table of contents entry

Photocatalytic ethanol dehydrogenation-acetalization to prepare value-added 1,1-dimethoxymethane and H_2 was achieved over non-precious metal CdS/Ni-MoS_2 catalytic under visible light. This work provides a promising strategy for atomic green economy application of bio-ethanol.

Keyword: visible light; non-precious metals; ethanol; photocatalytic; 1,1-diethoxyethane.

Yuguang Chao, Wenqin Zhang, Xuemei Wu, Nana Gong, Zhihong Bi, Yunqin Li, Jianfeng Zheng,* Zhenping Zhu and Yisheng Tan*

Visible light Direct Conversion of Ethanol to 1,1-Diethoxyethane and Hydrogen over Non-Precious Metal Photocatalyst